

Role of the precursor in a triple-pulse pumping scheme of a nickel-like silver soft-x-ray laser in the grazing-incidence-pumping geometry

K. A. Janulewicz* and C. M. Kim

Advanced Photonics Research Institute, Gwangju Institute of Science and Technology, Gwangju, 500-712, Korea

(Received 24 January 2010; revised manuscript received 8 August 2010; published 5 November 2010)

Soft x-ray lasers pumped in the grazing incidence geometry show strongly reduced energetic needs but hardly changed conversion efficiency between the pump energy and the output short-wavelength radiation. Numerical analysis presented in the paper concerns with performance of a Ni-like Ag soft-x-ray laser pumped by a triple-pulse structure in the grazing incidence geometry as a function of the pumping conditions. It was found that a weak precursor preceding the main preforming and heating pulses by a few nanoseconds is crucial for the energy deposition. Its presence enables in different arrangements a reasonable reduction in the pump energy and relaxation of the steep density gradients as well as a control over partition of the deposited energy. As a consequence, it was concluded that a well energetically balanced three- or multipulse composition seems to be a reasonable way to achieve performance improvement.

DOI: [10.1103/PhysRevE.82.056405](https://doi.org/10.1103/PhysRevE.82.056405)

PACS number(s): 52.50.Jm, 42.55.Vc, 32.30.Rj, 42.60.By

I. INTRODUCTION

There has been much progress recently in reducing energetic needs for pumping soft-x-ray lasers (XRLs). The major advance enabling saturated lasing at the wavelengths between 10 and 20 nm with a total pump laser energy as low as 1 J was possible owing to the grazing incidence pumping (GRIP) geometry [1–4]. The GRIP geometry was proposed [1] and demonstrated [2] for Ni-like molybdenum emitting at 18.9 nm. This result has been reproduced in the experiments reported in [3–5] confirming feasibility of the method. In spite of much lower pump energy the reported gain coefficient increased significantly in comparison to the traditional scheme of the normal incidence and achieved values between 50 and 80 cm⁻¹ [2,3,5–7]. This increase in the gain value was accompanied by gain lifetime shortening. Stable, saturated lasing with an output energy of about 1 μJ required a width of the focal line in the range of few tens of micrometers [3,4,7,8]. The major drawback of this arrangement is gain deterioration on the high-density-side of the gain volume as ionization time is roughly scaled with the electron density (n_e) as $\sim 1/n_e$ [9]. All these means and the progress achieved in reduction of the pump pulse energy did not result in significant improvement of the total conversion efficiency of the pump energy into the short-wavelength radiation. The latter was usually about a value of 10⁻⁶ and has been hardly changed. It means that GRIP still needs optimization and analysis of new experimental data to understand better how this scheme works and where the improvement possibilities exist.

Recently a very comprehensive analysis of the physical aspects of GRIP, including analytical models supported by some numerical results and scaling rules, has been presented in [9,10]. A set of the conditions necessary for efficient lasing has been formulated for each of two pump laser pulses as well as simple and direct criteria for gain optimization [9]. The analysis included also x-ray lasers working at wave-

lengths below 10 nm [10]. Very recently, these criteria were discussed in the context of the new pumping scheme applying single profiled pump pulse [11]. It was shown that the criteria formulated in [9] are most frequently fulfilled for the traditional double-pulse GRIP arrangement with the preforming laser pulse of normal incidence. However, the result of preforming at a very low energy level, typical for the single profiled pulse, strongly deviates from the commonly accepted picture. In this case, a significant part of plasma preforming has actually to be done within the duration of the leading edge of the main heating pulse and this fact changes the temporal scale of the analyzed processes. The untypical behavior is caused by the tenuous character of a preplasma enabling energy deposition at the critical surface during the initial phase of the main heating pulse. The plasma density profiles are determined rather by ionization than a strong expansion and are of moderate and nearly constant steepness across the whole plasma column [11].

As the double- and single-pulse pump schemes show some deficits discussed in [11], the question arises whether more complex or in different way temporally structured pump laser radiation is able to improve the performance by increase in the output level and beam quality. It is evident that in the described schemes a noticeable part of the delivered energy is deposited, at the different stages of the pump process, in the medium areas impracticable for lasing due to very strong refraction. The emitted and amplified short-wavelength radiation traversing these areas is very quickly bent out of the plasma column or at least of the area of noticeable gain. In some of the reported experiments on GRIP x-ray lasers the traditional double-pulse scheme was preceded by a weak precursor falling normally to the target [3,5,7,8,12]. These experiments belonged to the most successful delivering reproducible and of reasonable quality signal at a moderate or even low pump power. This fact has turned our attention to a triple-pulse structure of the pump scheme. The influence of the low-level preforming pulses (precursor+strong prepulse) on the plasma hydrodynamics and kinetics was investigated by numerical modeling in [13]. However, this work focused rather on the propagation effects

*kaj@gist.ac.kr

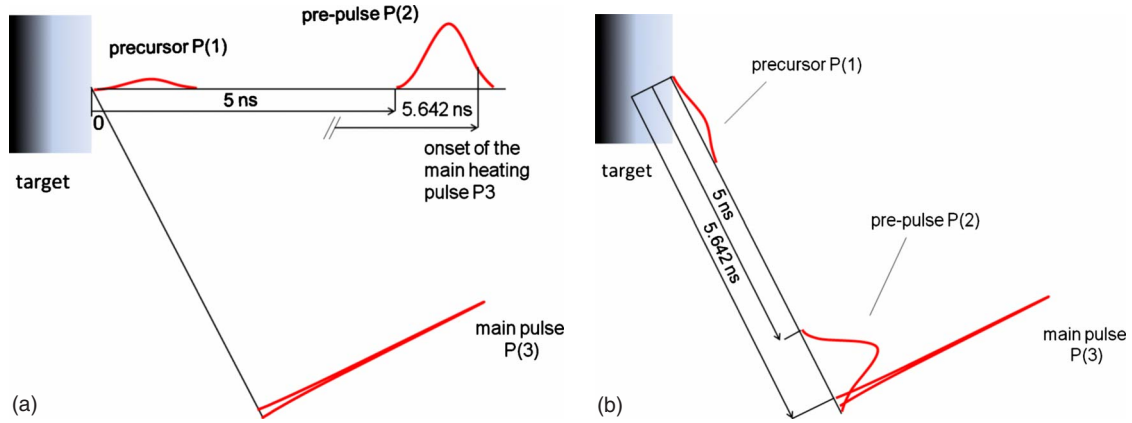


FIG. 1. (Color online) Two of the discussed arrangements in the triple-pulse pumping GRIP geometry. (a) The standard (most common in practice) irradiation scheme with the precursor and prepulse falling perpendicularly to the target surface; (b) pump pulse structure of irradiation in the all-GRIP geometry: all pulses are impinging on the target at a grazing angle. The corresponding pump energies are equal to: 15 mJ (P1), 263 mJ (P2) and 700 mJ or 560 mJ (P3). Both the precursor and prepulse have a width of 350 ps (FWHM) and a width (FWHM) of the main pulse is equal to 8 ps.

dependent on the plasma density gradients. A density valley accompanied by guiding was considered as a tool of energy extraction improvement. It was claimed that such structures can be created only if the second preforming pulse irradiates the plasma under grazing incidence angle. Our results do not confirm this conclusion.

In this paper we present and discuss results of numerical modeling performed to identify the effect of a precursor in the pump laser pulse structure on the system performance. Temporal dependence of the energy partition and the plasma parameters important for the medium kinetics constitute the measure for the precursor effect. A Ni-like Ag soft XRL emitting at 13.9 nm and pumped in the GRIP geometry is the object of our analysis. However, qualitative results or observed trends in behavior are also applicable to XRLs working with other ionic species pumped in the GRIP geometry and emitting at wavelengths above 10 nm. Identification of the processes supported by the precursor enables formulation of further search directions toward the pump pulse energy reduction and performance improvement.

II. MODEL

Modeling was conducted with the hydrodynamics/atomic physics numerical code EHYBRID dedicated to simulations of collisional x-ray lasers [14,15]. The code proved its reliability in some previous simulations of x-ray laser experiments [9,10,16,17]. Three well distinguishable, separate components are included into the structure of the incident radiation (Fig. 1). The pump laser beam at a wavelength of 800 nm irradiates the target being focused to a line of 7 mm length and 30 μm width—the values used in the simulations were taken close to the experimental conditions described in [11]. An incident energy of the main pulse is assumed to be equal to 700 mJ while the prepulse and precursor contained 263 and 15 mJ, respectively. It was found that a long delay of 5 ns (peak-to-peak) between the precursor and prepulse is favorable for the laser output. The main, short heating pulse is switched-on at the moment delayed 642 ps relative to the

beginning of the prepulse what gives a time gap between the peaks of both pulses equal to 300 ps. The main pulse has a Gaussian form with a width of 8 ps and a rise time of the leading edge is equal to the width. Precursor and prepulse are assumed to be also Gaussian pulses. This gives a linear irradiation density of 1.0 J/cm for the main pulse. The preforming part of the three-pulse scheme delivered linear energy density of 0.375 J/cm and the precursor of 0.0215 mJ/cm.

Modeling is focused on behavior in space and time of four most important parameters of the plasma used as an active medium: plasma density (n_e), electron temperature (T_e), average ionization stage (Z^*) and the local gain coefficient (g_0). It is evident, that the assumed irradiation conditions are in the preforming phase much more modest than those used in [9]. A nickel-like silver x-ray laser working at 13.9 nm has been chosen as the investigation object as this is the most popular scheme with the richest experimental data available. The output analysis has been extended by the information on partition of the deposited energy to strengthen the conclusion regarding the system performance. The considered forms of the deposited energy include the kinetic (E_{kin}), thermal (E_{therm}), ionization (E_{ionis}) and radiative (E_{rad}) components. The last one does not include the energy in the lasing transitions. The distribution of the total absorbed energy among different energy components is presented with normalization by value of the total incident energy. The EHYBRID code delivers an approximate energy content in each of these components at any time point and this is analyzed together with the medium kinetic data to conclude about the medium performance.

III. TRIPLE-PULSE ARRANGEMENT

The starting point of the analysis is the arrangement including prepulse and precursor incident normally (perpendicularly) to the target surface as in Fig. 1(a). A grazing incidence angle of the main pulse is assumed to be equal to 18° and the total pump energy is close to 1.0 J, the value applied frequently in the experimental work. The temporal

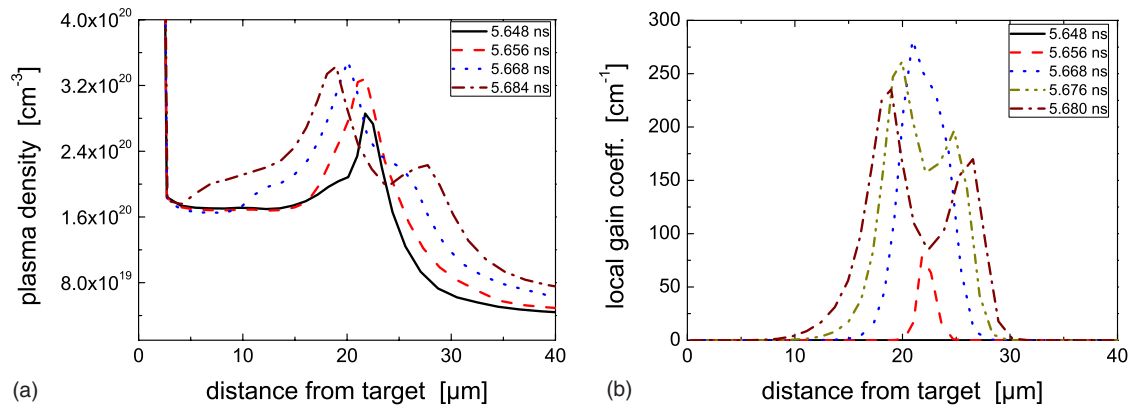


FIG. 2. (Color online) The history of the plasma density (a) and local gain coefficient (b) for the pump case using three separate pump pulses with a total energy of ≈ 1 J (0.7 J in the main pulse, 0.263 J in the prepulse and 15 mJ in the precursor) and both the precursor and prepulse falling on the target normally to its surface. The pre- and main pulses are delayed relative to the begin of the precursor by 5 and 5.642 ns, respectively.

characteristics of the precursor and prepulse were given earlier. The results for the plasma density and the local gain coefficient obtained under these irradiation conditions are shown in Figs. 2(a) and 2(b). Comparison between both figures makes it clear, that the highest gain is generated at the density ridge being the result of interaction between a solid target and the preforming combination of the precursor and prepulse.

This density ridge creates a kind of a barrier for the incident radiation and predetermines the place of the major energy deposition. The position of the high-gain area appears to be very stable in time while the gain coefficient distribution broadens only slightly and shows some strongly pronounced dip caused by strong and fast overionization in the primary deposition area. However, the high-gain area is shifted to the outer regions of the plasma plume if compared to the schemes with either single preforming pulse or a single profiled pulse and this is a positive feature of this arrangement. It is also clearly seen a kind of a density valley created in the late phase of gain generation [5.684 ns after the beginning of pumping or 34 ps after the main pulse peak, see Fig. 2(a)]. The high-gain area corresponds well to the optimum plasma density foreseen to be at 2×10^{20} cm^{-3} .

One major effect limiting energy extraction appears in this scenario. This seems to be very high temperature localized within a narrow spatial area by the pump process and its geometry. This requires disadvantageous waiting for spread of the stored energy over the significant part of the plume volume. Due to the long duration of this waiting phase the process is accompanied by a significant overionization level reducing quickly some part of the gain and leading to reduction in the energy stored in the medium and available for extraction. Not without a consequence for the output signal, as the increase in the overionization level will shorten the output pulse due to faster gain termination. On the other hand, it is also clear that such a system enabling free expansion of the preformed plasma (result of joint act by the precursor and prepulse) within some significant time gap reduces the energy losses to the bulk target, shifts gain area outwards the high density area and stabilizes the position of the gain area in time.

Another possible variant of the irradiation geometry is the situation with all laser pulses impinging on the target at a grazing angle [all-GRIP arrangement shown in Fig. 1(b)]. As the same level of the used energy could cause only increase in the density barrier level and increased absorption there,

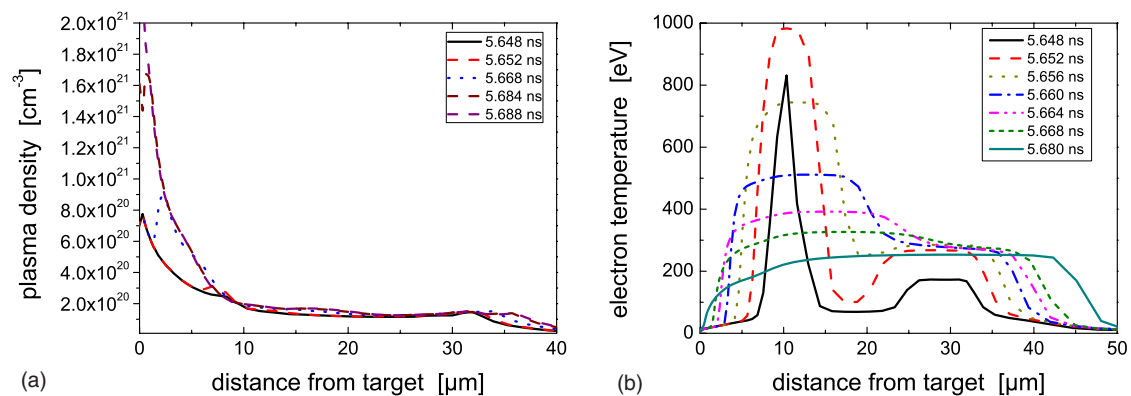


FIG. 3. (Color online) Time-resolved plasma density (a) and electron temperature (b) in plasma of the active medium for the pump case using three separate pump pulses but all falling under grazing angle on a target (all-GRIP configuration). The energy of the main pulse has been reduced to 560 mJ.

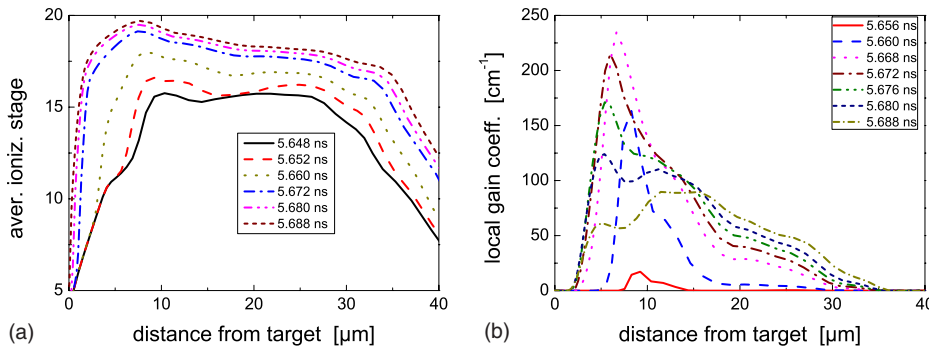


FIG. 4. (Color online) The history of the average ionization stage (a) and the local gain coefficient (b) in the medium of a Ni-like silver x-ray laser pumped in the all-GRIP arrangement.

the main pulse energy in this irradiation geometry has been reduced to the arbitrarily chosen level of 560 mJ (20%), keeping the precursor and prepulse energies unchanged. It was assumed that this will bring us back to the plasma behavior observed in the standard (normal to the target) preforming (Fig. 2). Interestingly, the plasma characteristics for this case are changed markedly (Figs. 3 and 4). Plasma density is slightly below the optimum level but it shows very well relaxed gradients in a broad area of the plume. There is no density ridge. This quite unexpected behavior can be explained with the plot demonstrated in Fig. 3(b). The electron temperature distribution shows in the case of all-GRIP arrangement initially two peaks that merge with elapsing time into a single broad one. As a result, the ionization distribution is broad and relatively uniform with a weakly pronounced maximum at high densities [Fig. 4(a)]. As a consequence, the gain distribution is also broad but with the peak noticeably closer to the target surface [Fig. 4(b)] and quickly reduced due to overionization. Such an electron temperature distribution suggests two deposition areas of the delivered energy. The prepulse energy is deposited in the area more distant from the target but of nearly gradientless density distribution and the incoming main pulse “percolates” through this region to deposit dominant part of its energy in more deeper part of the plasma plume characterized by strong increase in density.

We assume, that the energy percolation origins in the saturated character of the inverse bremsstrahlung (IB). First, IB depends strongly on the plasma density as $\sim n_e^2$ and on the electron temperature as $\sim T_e^{-3/2}$. Second, weak absorption combined with hardly existing density gradients cause the nonabsorbed energy at the primary position to penetrate the plasma plume deeper and to be absorbed dominantly at high density area close to the target surface. The effect is clearly caused by the irradiation geometry in the preforming phase as it exists also for higher main pulse energies in the same geometry but it is absent in the case of normally incident preforming pulses.

The question arises whether it is really an effect solely of the irradiation geometry. To check it, the same energetic composition of the pump radiation was kept unchanged, but the precursor (15 mJ) has been directed normally to the target surface. The effect of this action is clearly seen in Fig. 5. In this figure the distributions of density, ionization stage (multiplied by factor 10) and electron temperature at the moment of 2 ps before the main pulse peak are plotted for both geometrical arrangements. It is easily seen that normally in-

cident precursor (solid lines) cancels the effect of the double-deposition described previously. The reason for that seems to be well understood. Normally incident precursor deposits its energy definitely in the high density region and produces a reasonable amount of plasma. On contrary, the grazing incidence of the precursor causes its trailing part to be deflected on the density gradients generated by the leading edge and it results in the deposition of significant part of the preforming energy at lower density, reducing the amount of the ablated material converted into plasma. The length of the precursor is sufficient to observe a noticeable hydrodynamic movement of the plasma within its duration. The reduced amount of the plasma becomes tenuous due to expansion and shows hardly density gradients over a broad area of the plume. This supports the “percolation” scenario described earlier for heating by the main pulse. More detailed picture of the medium conditions when in the triple-pulse irradiation only the precursor falls normally to the target is given in Fig. 6. It becomes clear that precursor is crucial for medium pumping. First of all, it enables creation of a low-gradient density shelf while other parameters are close to those considered as the optimum in [9]. Hence, energy deposition is well localized in a noticeable distance from the target surface at the optimum density and moderate electron temperature. As a result, one can speak about efficient lasing and long-lived gain due to limited overionization. The density distribution shows weak flattening behind the weak first ridge—the structure very similar to that termed as a density valley in [13]. However,

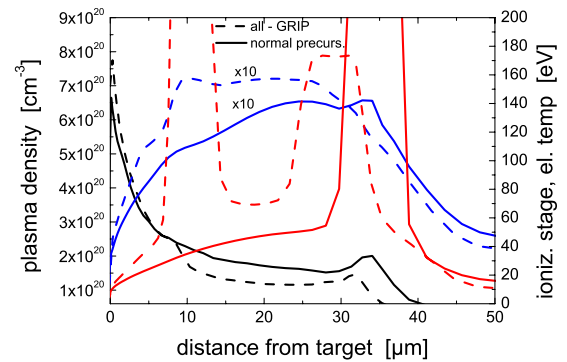


FIG. 5. (Color online) Plasma preforming by a combination of the precursor and prepulse in two arrangements with the same energetic content but different irradiation geometry. Difference relies on either normal or grazing incidence of the precursor. The values of the average ionization stage are strengthened by a factor of 10 to make the distribution better visible.

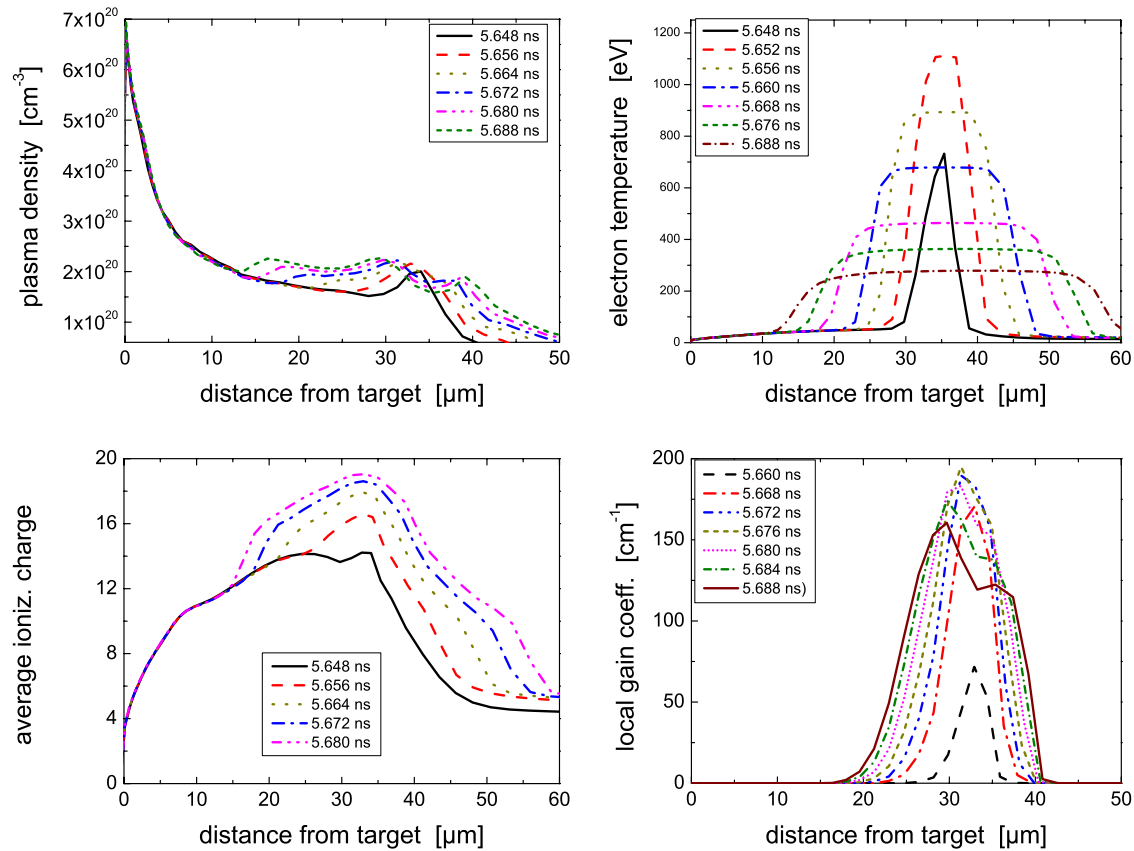


FIG. 6. (Color online) History of the plasma parameters of the medium pumped in the three-pulse arrangement with the precursor falling normally to the target. The main pulse energy is equal to the reduced value of 560 mJ.

more detailed look at the gain coefficient distribution reveals that the highest gain is not created at the density valley as suggested in [13] but it is slightly shifted toward the target and corresponds very well to the second weak density ridge. Such a behavior is understandable as the gain follows higher plasma density and, especially, the ionization stage closer to the required one. Moreover, as the density valley is placed between two weak density humps, the radiation crossing such a density profile will undergo a complex refraction effect. First, the incident beam will be deflected toward the target (the valley bottom) on the descending slope, then goes without significant direction change through the flat valley bottom to be subsequently refracted outwards the target surface on the opposite slope of the density dip. It is obvious that the perigee of the beam trace should be placed somewhere within the second density ridge and not at the valley bottom. In our case the density dip starts to be visible quite late, dominantly in the postpump phase. As the time scale of changes after onset of the heating laser pulse is short, and no noticeable changes in the density distribution character are observed, the density distribution modification seems to be result of the ionization process rather than any hydrodynamic movement. Ray-tracing results suggest gain-guided propagation rather than refraction index guiding suggested in [13].

Distribution of the deposited energy among its different forms in an active medium could be a reasonable additional check for the system performance under different irradiation conditions. It can give an indication which processes are pre-

ferred or dominant during the pump process and after its conclusion. The result presented in Fig. 7(a) reveals basic difference between the original double-pulse GRIP geometry (dashed lines) and the triple-pulse pumping scheme with preforming occurring under the normal incidence (solid lines) irradiation. Apart from the fact that the total energy of the double-pulse irradiation is lower by 15 mJ due to the non-existing precursor, the fundamental difference appears in the level of the kinetic energy of the plasma. The double-pulse irradiation gives significantly higher kinetic energy than that in the triple-pulse arrangement. That means, the ablation process is more dynamic in the case of normally incident single prepulse of a noticeable energy (263 mJ). Moreover, lower delivered energy does not mean lower absorbed energy, and on the contrary, the energy absorbed in the double-pulse scheme is slightly higher due to dominant deposition at the critical surface.

The new question arises about the energy partition under irradiation by three pump pulses in different geometrical arrangements. One variant includes the preforming pulses falling normally to the target surface (solid lines) while the another one is the all-GRIP geometry (dashed lines), both sketched in Fig. 1. The answer can be derived from the plots drawn in Fig. 7(b). First of all, the kinetic energy is left at a low level in both cases with the total absorbed energy very similar in both variants. On the other hand, the all-GRIP arrangement is characterized by faster decrease in the thermal energy accompanied by, what should be expected, in-

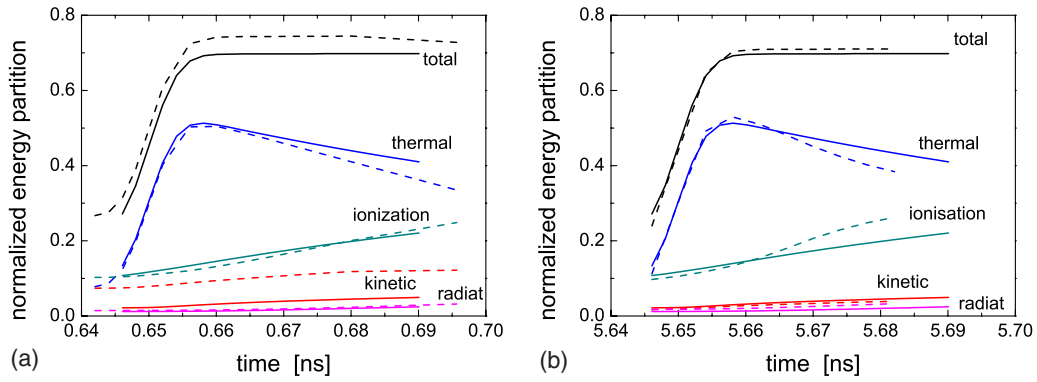


FIG. 7. (Color online) Energy partition normalized to the total delivered energy for: (a) three-pulse arrangement with the preforming pulses falling normally to the target surface (solid) and two-pulse (prepulse+main pulse) GRIP (dashed); (b) three-pulse arrangement with both preforming pulses falling normally to the target (solid) and at grazing angle (dashed).

crease in the ionization component. These two forms of the internal energy are closely related. For the sake of completeness it is necessary to check if the situation in the plasma behavior observed for the normally falling precursor is also reflected in the energy partition. The energy distribution among the components in such a case is shown in Fig. 8. The data for the normally incident precursor are plotted with dashed lines and it suggests slightly lower absorbed energy, higher thermal energy in the late phase of the excitation process and the corresponding reduction in the ionization energy caused by less intense ionization in the beginning of the excitation process when the thermal energy was lower as a result of weaker absorption. This exactly reflects the observations on the plasma parameters sketched earlier and suggesting a stable and long-lived gain due to limited overionization. The kinetic and radiative energies are very low and at a similar level. This observation of the deposited energy redistribution turns again ones attention to the role of the precursor in the pumping process. It seems to be obvious, that the precursor works as a source of an inhibition mechanism for the energy deposition in the high density region. It is beneficial if it impinges on the target normally as then it

creates denser primary plasma in a well developed column of weak density gradients. The latter is, in fact, the result of long temporal gap between the precursor and the more energetic prepulse (here 5 ns). This primary plasma column works as an absorbing buffer even for the normally incident more energetic prepulse assuring reduced kinetic energy of the generated plasma medium. The prepulse incident on this primary plasma under a grazing angle is more effective in heating due to increased absorption/interaction length. This gives increase in the thermal energy, intensifies collisional ionization process and reducing in turn the part of the thermal energy available (Fig. 8).

IV. SUMMARY

It was shown that more complex pump laser pulse structure has potential to be more efficient one and to enable significant reduction in the energy of the main pulse. The triple-pulse irradiation geometry analyzed here in detail and successful in the experiment confirmed its advantages also in the numerical simulations. The analyzed structure is not the only one but it suggests rather a trend in the further development leading to more efficient conversion of the pump energy available. By dedicated structuring of a pump pulse consisting of three components it was possible to reduce the losses connected with the thermal conduction to the bulk material as well as to avoid creation the high-gain area at high densities associated usually with steep density gradients and very strong refraction effects. This explanation differs in the main aspect from that offered in [12,13]. The latter was concentrated mainly on relaxing the density gradients and the refraction-based limitations. In spite of this, the general hydrodynamics picture presented here is similar to that reported in [13]. It is also shown that the amount of energy included in the preforming phase and heating has to be well balanced to work toward improvement of the output parameters. In other words, the amount of the generated preplasma should match the heating potential of the main pulse. In the presented analysis, consideration of the optimum grazing angle was neglected for two reasons. The dependence of the preplasma behavior on the pump laser pulse structure suggests that all analyses regarding the general optimum inci-

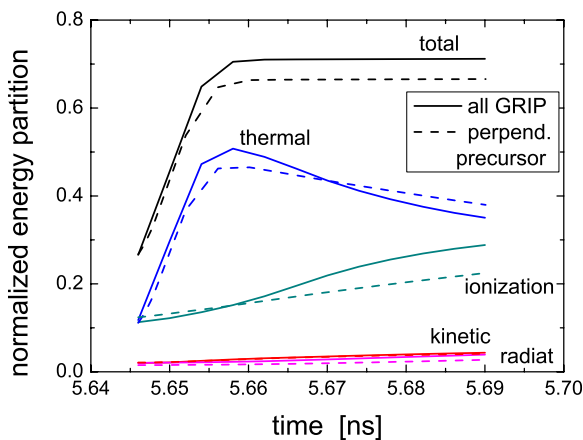


FIG. 8. (Color online) Energy partition normalized by the total delivered energy for the three-pulse all-GRIP arrangement (solid) and with only precursor impinging perpendicularly on the target (dashed).

dence angle are spurious as every pump scheme can give different values depending on the pump pulse structure. On the other hand, the observed in the experiment output dependence on the incidence angle, under specific irradiation conditions, is broad with a weakly pronounced maximum. It was also found that amplification in a system pumped by one of the described methods works rather in the gain-guiding regime and can lead to spatially very narrow output beam and elongated pulse duration. It was not our goal to predict or reproduce the experimental results with a high accuracy. It is rather about explanation how the system works under given

conditions and to indicate some possible ways for the further progress.

ACKNOWLEDGMENTS

The authors express their gratitude to Professor Geoff Pert of the York University for invaluable discussions on the topic and his support in using EHYBRID code. The work presented here was supported by the research project Photonics 2020 through a grant provided by the Gwangju Institute of Science and Technology in 2009 as well as by the GIST Dasan Fund.

-
- [1] R. Keenan *et al.*, *Proc. SPIE* **5197**, 213 (2003).
 [2] R. Keenan, J. Dunn, P. K. Patel, D. F. Price, R. F. Smith, and V. N. Shlyaptsev, *Phys. Rev. Lett.* **94**, 103901 (2005).
 [3] B. Luther, Y. Wang, M. A. Larotonda, D. Alessi, M. Berrill, M. C. Marconi, J. J. Rocca, and V. N. Shlyaptsev, *Opt. Lett.* **30**, 165 (2005).
 [4] J. Tümmler, K. A. Janulewicz, G. Priebe, and P. V. Nickles, *Phys. Rev. E* **72**, 037401 (2005).
 [5] Y. Wang, M. A. Larotonda, B. M. Luther, D. Alessi, M. Berrill, V. N. Shlyaptsev, and J. J. Rocca, *Phys. Rev. A* **72**, 053807 (2005).
 [6] H. T. Kim *et al.*, *Phys. Rev. A* **77**, 023807 (2008).
 [7] K. Cassou *et al.*, *Opt. Lett.* **32**, 139 (2007).
 [8] J. J. Rocca, Y. Wang, M. A. Larotonda, B. M. Luther, M. Berrill, and D. Alessi, *Opt. Lett.* **30**, 2581 (2005).
 [9] G. J. Pert, *Phys. Rev. A* **73**, 033809 (2006).
 [10] G. J. Pert, *Phys. Rev. A* **75**, 023808 (2007).
 [11] A. Janulewicz, C. M. Kim, H. T. Kim, and J. Lee, in *X-Ray Lasers 2008*, Proc. of the 11th International Conference on X-ray Lasers, 17–22 August 2008 Belfast, UK, edited by C. L. S. Lewis, D. Riley (Springer, New York, 2009), p. 81.
 [12] S. Kazamias *et al.*, *Phys. Rev. A* **77**, 033812 (2008).
 [13] J. Zhao, Q. L. Dong, and J. Zhang, *Opt. Lett.* **32**, 491 (2007).
 [14] P. B. Holden, S. B. Healy, M. T. M. Lightbody, G. J. Pert, J. A. Plowes, A. E. Kingston, E. Robertson, C. L. S. Lewis, and D. Neely, *J. Phys. B* **27**, 341 (1994).
 [15] G. J. Pert, *J. Fluid Mech.* **131**, 401 (1983).
 [16] K. A. Janulewicz, J. Tümmler, G. Priebe, and P. V. Nickles, *Phys. Rev. A* **72**, 043825 (2005).
 [17] K. A. Janulewicz, P. V. Nickles, R. E. King, and G. J. Pert, *Phys. Rev. A* **70**, 013804 (2004).